

WATERMARK RE-SYNCHRONIZATION USING LOG-POLAR MAPPING OF IMAGE AUTOCORRELATION

Adnan M. Alattar[†] and Joel Meyer[‡]

Digimarc Corporation
19801 SW 72nd Ave., Suite 250
Tualatin, OR 97062

[†]aalattar@digimarc.com, [‡]jmeyer@digimarc.com

ABSTRACT

Many watermarking algorithms embed the watermark into the image as contiguous non-overlapping tiles. This tiling structure forms an implicit synchronization template that can be revealed through autocorrelation. This template is composed of a set of weak peaks, replicating the relative position of the watermark tiles. Hence, synchronization can be resolved by comparing the actual locations of these peaks to the theoretical ones to determine the scaling factor and the orientation angle of the tiles. Unfortunately, these peaks are very weak and measuring their locations directly is not easy. In this paper, a log-polar mapping of the synchronization template is computed to convert the scaling factor and the rotation angle of the template into vertical and horizontal shifts. These shifts are then detected using a Phase-Only-Matched filter (POM), which concentrates the weak energy from all peaks into a single peak that is much easier to detect. The scaling factor and orientation angle are determined from the location of this peak. Simulation results of this method have shown that this method is very effective and produces accurate results.

1. INTRODUCTION

Watermarking is the technique of hiding imperceptible information in media such as image, video, and audio. Due to its many important applications, watermarking has become an important field during the past decade. Its applications include authentication, copyright protection, fingerprinting, video monitoring, connected media, and device control [1]. In most of these applications, the media undergoes unintentional manipulations and processing that usually cause a change in the scale and rotation of the watermarked media. Moreover, in many of these applications, attackers may attempt to defeat the watermark as a security feature by intentionally changing the scale and rotation of the media. Therefore, a robust watermarking system must be capable of re-synchronizing itself against scaling and rotation.

The use of an exhaustive search is the easiest, but most computationally intensive and hence most time-consuming, method of geometric synchronization. The

template approach, however, has the potential to provide a more efficient geometric synchronization. It uses an explicit, but hidden, synchronization template to guide the resynchronization process [2]. In some implementations, the template is a constellation of peaks embedded in the magnitude of the Fourier transform of the media. The Fourier magnitude rotates and shrinks/expands according to the rotation and scaling of the original image. Hence, the rotation angle and the scaling factor can be easily determined from the template. The Fourier-Mellin transform has been used to convert the scaling factor and rotation angle into horizontal and vertical shifts [3]. Also, a POM has been used to effectively detect these shifts [3]. As with other approaches, this approach forces a trade-off between robustness and capacity of the watermark due to the allocation of energy between synchronization and variable message portion of the watermark.

A self-synchronizing watermark has been proposed as another method for geometric synchronization [4]-[6]. In this approach, a pseudo-random watermark is tiled over the image in a non-overlapping fashion. The tiling structure forms an implicit template that can be revealed by computing the autocorrelation of the image. In this case, the autocorrelation function contains a regular pattern of peaks, replicating the relative position of the watermark tiles. By comparing the actual locations of these peaks with the theoretical ones the synchronization can be resolved. Unfortunately, these peaks are very weak, and detecting them is not easy.

Kutter [4] and Su and et. al. [5] suggested boosting the energy in these peaks using the gradient operation. Deguillaume and et. al. [6] avoided the detection of these peaks by detecting the periodic behavior of the power spectrum using a Hough transform.

In this paper, we propose to detect the autocorrelation peaks of the self-synchronizing watermark through a process similar to that used with the explicit template approach described above. For this purpose, a log-polar mapping of the autocorrelation image is computed to convert the scaling factor and the rotation angle into vertical and horizontal shifts. These shifts are then detected using a Phase-Only-Matched filter, which

concentrates the weak energy from all peaks into a single peak that is much easier to detect.

2. AUTO-CORRELATION

The watermark $w(x,y)$ is embedded in the spatial domain of the host image $I(x,y)$ (of size $X \times Y$) as follows:

$$I_w(x,y) = I(x,y) + g(x,y)w(x,y) \quad (1)$$

where $g(x,y)$ is an adaptive gain, which is used to reduce image distortion while maximizing watermark detection.

The watermark $w(x,y)$ is constructed by repeating an elementary watermark tile $\hat{w}(x,y)$ (of size $K \times L$) in a non-overlapping fashion, such that it covers $I(x,y)$.

The watermark can also be embedded in the magnitude of the Fourier transform of $I(x,y)$ as follows:

$$\|\mathfrak{F}(I_w(x,y))\| = \|\mathfrak{F}(I(x,y))\| + g(u,v)w(u,v) \quad (2)$$

where $\mathfrak{F}(\cdot)$ represents the 2-D Fourier transform and $\|\cdot\|$ is the magnitude operator.

The autocorrelation function $\eta(m,n)$ of the watermarked image $I_w(x,y)$ can be expressed as follows:

$$\eta(m,n) = \sum_{x=0}^{X-1} \sum_{y=0}^{Y-1} I_w(m,n)I_w(m+x,n+y) \quad (3)$$

When equation (1) is substituted in the above equation, $\eta(m,n)$ can be written as:

$$\begin{aligned} \eta(m,n) = & \sum_{x=0}^{X-1} \sum_{y=0}^{Y-1} I(m,n)I(m+x,n+y) + \\ & \sum_{x=0}^{X-1} \sum_{y=0}^{Y-1} g(m,n)w(m,n)g(m+x,n+y)w(m+x,n+y) + \\ & \sum_{x=0}^{X-1} \sum_{y=0}^{Y-1} g(m,n)w(m,n)I(m+x,n+y) + \\ & \sum_{x=0}^{X-1} \sum_{y=0}^{Y-1} I(m,n)g(m+x,n+y)w(m+x,n+y) \end{aligned} \quad (4)$$

The cross-correlation terms (last two terms) of the above equation can be ignored, since the watermark can be safely assumed to be uncorrelated with the host image. In this case, the autocorrelation function can be simplified to

$$\eta(m,n) \cong \phi(m,n) + \psi(m,n) \quad (5)$$

where $\phi(m,n)$ is the autocorrelation function of the host image and $\psi(m,n)$ is the autocorrelation function of the scaled watermark $w(x,y)$. If $\hat{w}(x,y)$ is designed to be uncorrelated random noise, its autocorrelation function will be a delta function. This causes peaks to occur in the autocorrelation function $\psi(m,n)$ exactly at locations corresponding to the relative offsets of watermark tiles $\hat{w}(x,y)$. The constellation formed by these correlation peaks forms a template that can be exploited for re-synchronization.

Applying a linear transformation A to $I_w(x,y)$ causes the autocorrelation coefficients $\eta(x,y)$, thus the peaks, to move to new locations (x',y') according to the equation:

$$\begin{bmatrix} x' & y' \end{bmatrix}^T = A \begin{bmatrix} x & y \end{bmatrix}^T \quad (6)$$

For a uniform scaling by factor S and a counter clockwise rotation by angle θ , A is given by:

$$A = \begin{bmatrix} S \cos \theta & -S \sin \theta \\ S \sin \theta & S \cos \theta \end{bmatrix} \quad (7)$$

It should be noted that in the case of frequency domain watermark embedding, according to equation (2), the autocorrelation function $\eta(m,n)$ must be computed using $\|\mathfrak{F}(I_w(x,y))\|$, instead of $I_w(x,y)$. In this case, the assumption that the watermark is not correlated with the host image is more applicable. This is because the coefficients resulting from the Fourier transform are normally de-correlated and the energy is concentrated on a few coefficients. This makes the FFT coefficients less correlated with the pseudo-random watermark. It also reduces image interference with the correlation peaks.

3. LOG-POLAR MAPPING

Transforming the Cartesian coordinates of equation (6) into polar coordinates using $x = \rho \sin \alpha$, $y = \rho \cos \alpha$ and $x' = \rho' \sin \alpha'$, $y' = \rho' \cos \alpha'$, and substituting equation (7), the following equation can be obtained:

$$\begin{bmatrix} \rho' \cos \alpha' \\ \rho' \sin \alpha' \end{bmatrix} = S \rho \begin{bmatrix} \cos(\alpha + \theta) \\ \sin(\alpha + \theta) \end{bmatrix} \quad (8)$$

The above equation suggests that if the autocorrelation function is re-sampled using log-polar mapping, the following results can be obtained:

$$\begin{bmatrix} \alpha' \\ \log \rho' \end{bmatrix} = \begin{bmatrix} \alpha \\ \log \rho \end{bmatrix} + \begin{bmatrix} \theta \\ \log S \end{bmatrix} \quad (9)$$

where the origin of the log-polar mapping is chosen at the center of the image. Equation (9) converts any rotation in the watermarked image into a shift in the horizontal axes. The magnitude of this shift exactly equals the rotation angle. Similarly, it converts any scaling in the image into a shift in the vertical axes. The magnitude of this shift exactly equals the log of the scaling factor. These two linear shifts in log-polar domain can be detected using the following POM:

$$\xi(m,n) = \mathfrak{F}^{-1} \left(\frac{\mathfrak{F}(LP(\eta(m,n)))^* \mathfrak{F}(LP(\phi(m,n)))}{\|\mathfrak{F}(LP(\eta(m,n)))\|} \right) \quad (10)$$

where “*” denotes the complex conjugate, $LP(\cdot)$ is the log-polar mapping and $\phi(m,n)$ is the autocorrelation of the embedded watermark before rotation and scaling, which can be easily generated by creating a hypothetical pattern with zeros everywhere and with ones at the expected peak

locations. The $\xi(m,n)$ represents the output of the POM filter, which contains a peak at the location (m_0, n_0) . The scaling factor, S , and the rotation angle, θ , are related to the values of m_0 and n_0 as follows:

$$S = \begin{cases} e^{-m_0} & m_0 \leq X/2 \\ e^{X-m_0} & m_0 > X/2 \end{cases} \quad (11)$$

$$\theta = n_0$$

where X is the height of the log-polar mapped image.

4. IMPLEMENTATION AND SIMULATION RESULTS

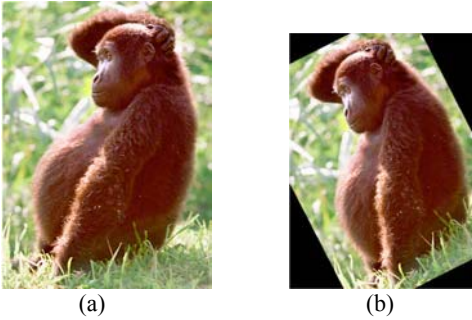


Figure 1. (a) Original watermarked image (b) Watermarked image rotated 27° counter clockwise then scaled 0.91%.

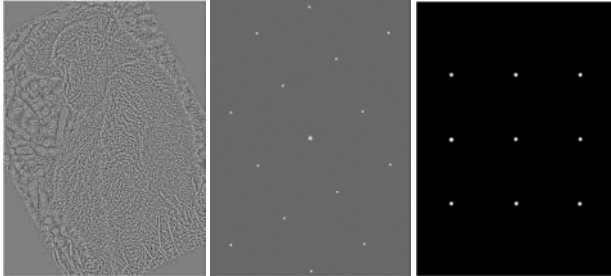


Figure 2. (a) The watermarked image after filtering with a high-pass non-linear filter, (b) the autocorrelation function of the image in Figure 2.a, and (c) a hypothetical autocorrelation function representing the unrotated-unscaled watermark.

We implemented the method described above and tested it with a watermarking algorithm similar to Digimarc's ImageBridge™. The watermark tiles in this algorithm are square (i.e. $K=L$). The exemplary image (600x432) shown in Figure (1.a) was watermarked and then rotated 27° counter-clockwise and scaled by a factor of 0.91 using Matlab. The resulted image is shown in Figure (1.b).

Before computing the autocorrelation function $\eta(m,n)$, the image in Figure (1.b) was processed using a non-linear high pass filter in order to remove the host image and hence improve the signal to noise ratio. The filtered image is shown in Figure (2.a). The image in Figure (2.a) was then doubled in both dimensions by padding it with zeros, before computing the autocorrelation function using the FFT. The zero padding is necessary in order to compute the linear instead of the circular correlation. The resulting

autocorrelation function is shown in Figure (2.b). To improve viewing after printing, all peaks in the figure have been manually exaggerated. The implicit template and its weak peaks can be observed in the figure.

Figure (2.c) shows a hypothetical autocorrelation function representing the image before rotation and scaling. The figure represents nine watermark tiles at the center of the image. This minimum number of tiles was chosen in order to reduce the effect of the noise from the host image and in order to reduce the ambiguity due to the cyclic nature of the pattern template in the autocorrelation image.

When Figure (2.b) is compared with Figure (2.c), it can be observed that the center portion of the template in Figure (2.b) is a rotated and scaled version of that in Figure (2.c). The rotation angle between the two templates is 27° counter-clockwise, and the distances between the peaks in Figure (2.b) are slightly shorter than those in Figure (2.c).

The log-polar mappings of the images in Figures (2.b) and (2.c) are shown in Figures (3.a) and (3.b), respectively. Again, the peaks in these figures were exaggerated for the purpose of better viewing after printing. The angle coordinate is plotted on the horizontal axis, and it was sampled at a rate of one sample per degree. The radial coordinate is plotted on the vertical axis and it was sampled such that $\sqrt{2} \times 256$ samples fall in half the maximum of the width and length of the image. Hence, the images in the figure are 362x360 pixels. Also, in computing the log-polar, we attempted to reduce the effect of the autocorrelation of the host image by excluding a small area around the origin. As seen in Figure (2.b), this area has high energy that decays away from the center. This energy is mainly due to the host image and can give no information about the tile relative locations.

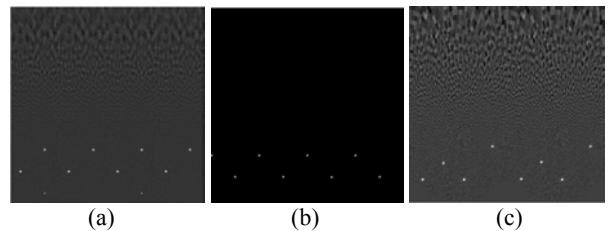


Figure 3. The log-polar mapping of the autocorrelation function (a) in Figure 2.a, (b) in Figure (2.b), and (c) of a watermarked image embedded with 128x100 random pattern watermark tile.

By comparing figures (3.a) and (3.b), a horizontal (left) and vertical (up) shifts can be observed between the patterns in these figures. These shifts are due to scaling and rotating the watermarked image. The vertical and horizontal distances between the peaks in the pattern are related to the dimensions (K and L) of the tile. When K does not equal to L , the pattern becomes less regular than it is in Figure (3). The log-polar mapping of the autocorrelation function of a watermarked image

embedded with a 128x100 random pattern watermark tile is shown in Figure (3.c).

The output $\xi(m,n)$ of the POM filter is shown in Figure (4.a), which shows several high energy peaks. These peaks are due to the cyclic nature of the pattern in Figure (3), and each of them corresponds to one of the 8 nearest neighboring watermark tiles. The energy in these peaks is several times that of the peaks in Figure (2.b), so they are much easier to detect.

As it is the case with the other peak finding methods used with the autocorrelation technique, the values of the measured scale and rotation may have some ambiguity [4]-[6]. This ambiguity is due to the regularity of the autocorrelation peaks, and it is limited to a factor of $\sqrt{2}$ in the scale and a multiple of 45° shift in the rotation angle. Hence, it can be resolved by trial and error during the reading stage of the watermark. The ambiguity can also be reduced to a 180° shift in the rotation angle by using a non-square ($K \neq L$) watermark tile. In this case, the pattern in the log-polar image becomes less regular (see Fig. (3.c)), and the POM filter produces two strong peaks separated by 180° and several other weaker peaks. One of the strong peaks is the correct peak. Figure (4.b) shows this case for a 128×100 random pattern watermark tile.

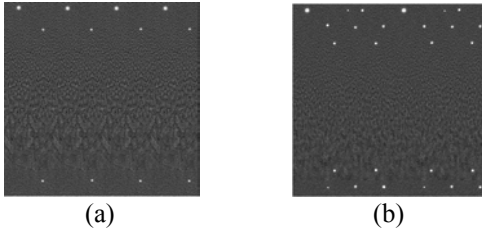


Figure 4. The result of the POM filter when applied to (a) the image in Figure (3.a) and (b) the image in Figure (3.c).

Finally, the location of the 12 highest peaks in Figure (4) was measured and used in equation (11) to calculate the scale factor and orientation angle. The correct scale and orientation was observed to correspond to the highest peak. The above process was repeated with various combinations of rotations and scales. The tested rotation angles are $0, \pm 37, \pm 65, \pm 90, \pm 135, \pm 161$, and the tested scale factors are 0.75, 0.85, 0.95, 1, 1.05, 1.15, 1.25. For every combination of rotation and scale, the highest 12 peaks were detected in the log-polar image, and the corresponding rotation angles and scale factors were determined.

In order to compare the accuracy of the proposed method, we compared it to the peak finding method suggested in [4] and [5]. We also detected the highest 12 peaks close to the image center and calculated the corresponding orientations and scales. We then used the closest rotation and scale to the true rotation and scale in order to calculate the average detection error (*ADE*). Similarly, we

calculated the *ADE* for our proposed log-polar method. The *ADE* is defined by equation (12):

$$ADE = \frac{1}{N} \sum_{n=1}^N \sqrt{(S_{\text{actual}} - S_{\text{detected}})^2 + (\theta_{\text{actual}} - \theta_{\text{detected}})^2} \quad (12)$$

The average *ADE* for our log-polar method was found to be 0.002479, while for the peak finding method suggested in [4] and [5], the *ADE* was 0.176861. This indicates that the log-polar method is more accurate than that suggested in [4] and [5]. The main cause of the inaccuracy in the peak finding method is due to the gradient calculation, which is used to boost the energy in the peaks before detecting them. This calculation tends to slightly shift the locations of the peaks. The accuracy of the log-polar method comes at the expense of an increase in computation due to the bi-cubic interpolation used in computing the log-polar mapping. Also, the log-polar method is applicable only when the scale is uniform.

5. CONCLUSIONS

A new method of determining the scale factor and the orientation angle of a watermarked image was proposed for watermarking algorithm that tiles the watermark over the image. The new method concentrates the energy of all peaks into a small set of peaks that can be easily detected. Simulation results indicated that this technique is more accurate for uniform scale but requires more computation than a typical peak finding technique. They also indicated that rectangular watermark tiles are more suitable for the proposed technique than square tiles.

6. REFERENCES

- [1] Ingemar Cox, Matthew Miller, Jeffrey Bloom, *Digital Watermarking*, Morgan Kaufmann Publishers, Oct 2001.
- [2] Shelby Pereira and Thierry Pun, "Fast Robust Template Matching For Affine Resistant Image Watermarking," in *International Workshop on Information Hiding*, Dresden, Germany, pp. 200-210, Sep 29-Oct 1, 1999.
- [3] Geoffrey B. Rhoads, "Methods for Surveying Dissemination of Proprietary Empirical Data," *U.S. Patent No. 5,862,260*, filed May 16, 1996 and issued January 19, 1999.
- [4] M. Kutter, "Watermarking Resisting to Translation, Rotation and Scaling," *Proc. of SPIE: Multimedia Systems and Applications*, vol. 3528, pp. 423-431, Boston, Nov 1998.
- [5] Po-Chyi Su and C.-C. Jay Kuo, "An Image Watermark Scheme to Resist Generalized Geometrical Transformations," *Proc. of SPIE: Multimedia Systems and Applications III*, vol. VV08, Boston, USA, Nov 2000.
- [6] F. Deguillaume, S. Voloshynovskiy, and T. Pun, "A Method for the Estimation and Recovering from General Affine Transform in Digital Watermarking Applications *Proc. of SPIE: Security and Watermarking of Multimedia Contents IV*, vol. 4675, pp.313-322, San Jose, Jan 2002.